Barrier RF Stacking Study

1. Goals:

- Near term - To increase proton intensity (protons per second, or pps) on the p-bar target by 50%:
  - Present: 4.5e12 protons every 1.467 seconds (22 Booster cycles).
  - Stacking goal: 9e12 protons every 2 seconds (30 Booster cycles).
- Medium term - To increase proton intensity (protons per second, or pps) on the NuMI target by 60%:
  - MI baseline: 3e13 protons every 1.867 seconds (28 Booster cycles).
  - Stacking goal: 6e13 protons every 2.333 seconds (35 Booster cycles).

2. Status as of September 2002:

- Paper study is finished. Main results:
  a. Can stack 2 Booster batches into the size of one Booster batch in the MI for p-bar production.
  b. Can stack 12 Booster batches into the size of six Booster batches in the MI for NuMI.
  c. Longitudinal emittance blow-up is about a factor of 3 (from 0.1 eV-s to 0.32 eV-s).
  d. Key issue is that the Booster beam must have a small $\Delta p/p$ to start with (required ΔE about ± 6 MeV).
  e. Compared with the slip stacking (another proposed scheme), one main advantage of the barrier rf stacking is smaller beam loading effects thanks to lower peak beam currents.
- Beam experiments and hardware are in preparation.

3. Experiments in the Recycler:

- Goal: To verify the simulation results.

- Recycler proton beam: 4 bunches (2.5 MHz) per injection from the MI. Longitudinal emittance = 2.5 eV-s per bunch. Assuming parabolic distribution, this gives ±4.7 MeV in energy spread.
- Recycler wideband rf: 2 kV maximum.
- Two experiments:
  a. Beam squeezing at various barrier bucket moving speed.
  b. Stacking using off-momentum injected beams.
- Key parameter $\Delta p/p$ measurement:
  a. Schottky spectrum:
     - ➢ Doable for unbunched beams.
     - ➢ Difficult for bunched beams.
     - ➢ Our case is somewhat in between: The beam is debunched (no synchrotron oscillation), whereas there is a strong coherent gap signal.

  b. Bucket scanning.

4. Experiments in the Booster:

- Goal: To obtain small $\Delta p/p$ beam at Booster extraction.
- Experiments:
  a. To suppress coupled bunch instabilities:
     - ➢ Feedback - Longitudinal damper. (D. Wildman)
     - ➢ Landau damping - To operate one rf cavity at h=83.

  b. To lower $\Delta p/p$ of the beam at extraction:
     - ➢ Bunch rotation.
     - ➢ Adiabatic compression.

5. Hardware Development:

1) Barrier rf system for the MI:
   - Goal: To build an 8-10 kV barrier rf system using Finemet cavities and high voltage fast switches.
   - Cavity: Based on the design of an rf chopper that was built by a Fermilab-KEK collaboration through a US-Japan Accord. Hitachi Metals will supply the Finemet cores.

- Switch circuit: Also based on the design of the rf chopper. Behlke will supply the switches (solid state HTS series). However, there is an important difference between the chopper circuit and the barrier rf circuit. The former uses a pair of +V and -V pulses. The latter requires a zero-voltage gap between +V and -V pulses. Therefore, the circuit needs to be modified.

2) MI rf modification: (J. Griffin)

- Goal: To reduce the beam loading effect by a factor of 3-4.
- Method: To lower the screen voltage from +2 kV to -100 V.

Barrier RF Stacking for NuMI 6-Batch Operation (B. Ng)

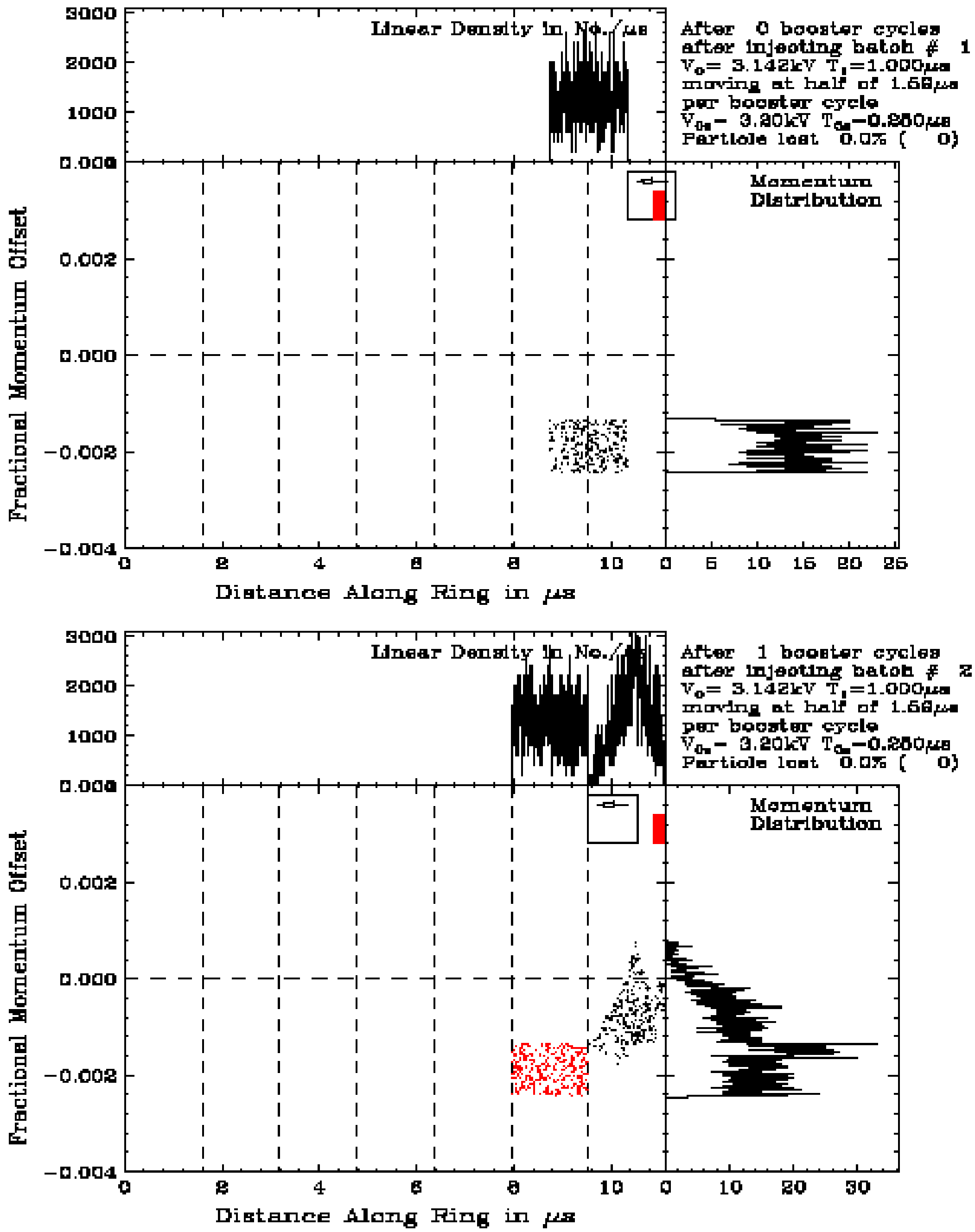

Figure 6: (color) Top: First batch (black) is injected between $5.5T_b$ and $6.5T_b$ with the right side touching the left side of the moving barrier, illustrated as an unfilled box with an arrow. Bottom: After one booster cycle, all particles in the first batch have just cleared the left side of the moving barrier, which is at $6.0T_b$. The second batch (red) is now injected between $5.0T_b$ and $6.0T_b$. Moving barrier has width $T_1 = 1.0\,\mu s$ and strength $V = 3.1421$ kV. Vertical dashed lines are spaced at T_b.

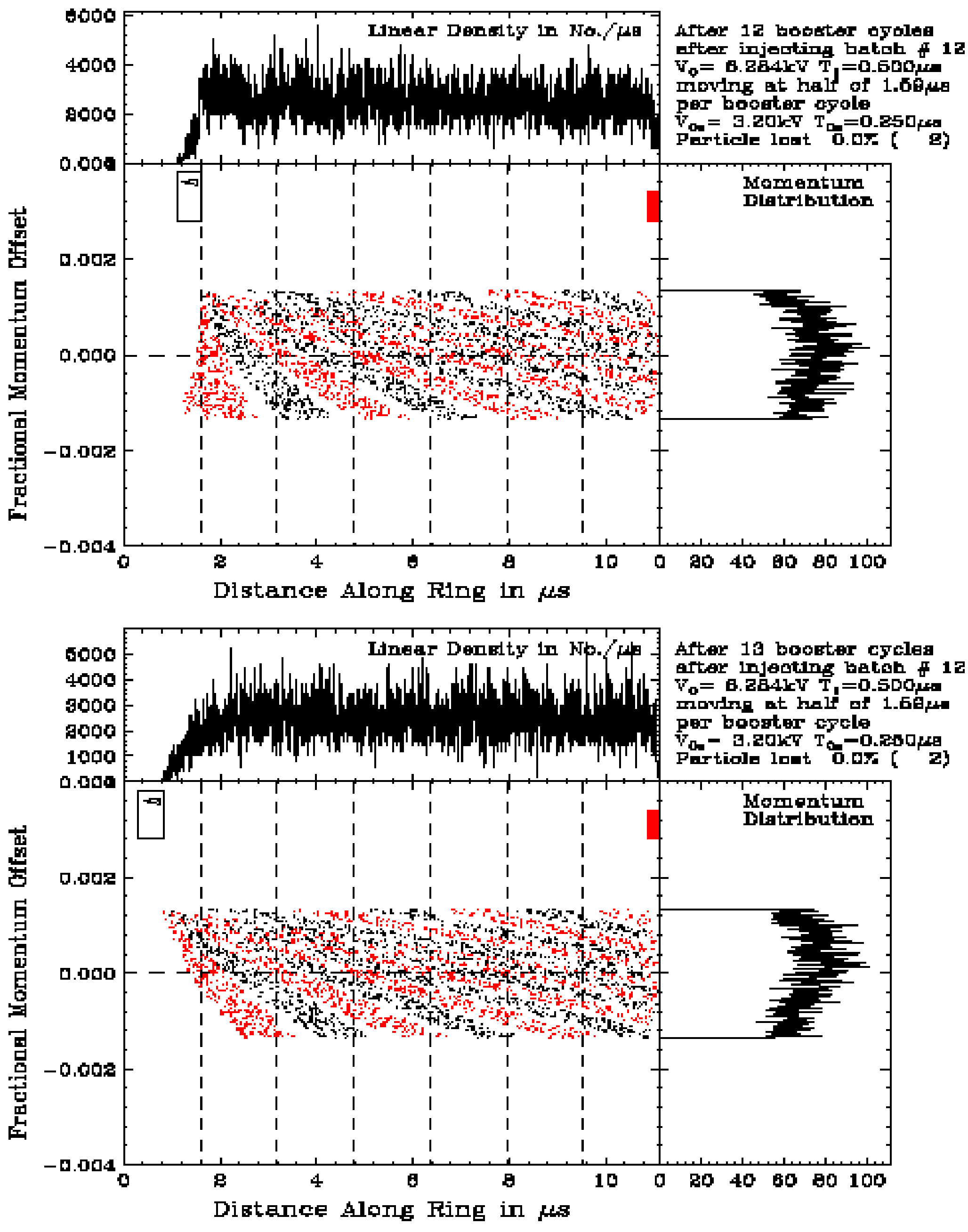

Figure 8: (color) Same as Fig. 7, but with the width of the moving barrier reduced to 0.5 μs and strength increased to 6.2842 kV. At injection of first batch, left side of barrier was placed at $6.7T_b$. Top: One booster cycle after the injection of the 12th batch between $0.2T_b$ and $1.2T_b$, or 12 booster cycles after the injection of the first batch. Bottom: Another booster cycle later.

Barrier RF Stacking for p-bar 2-Batch Production (B. Ng)

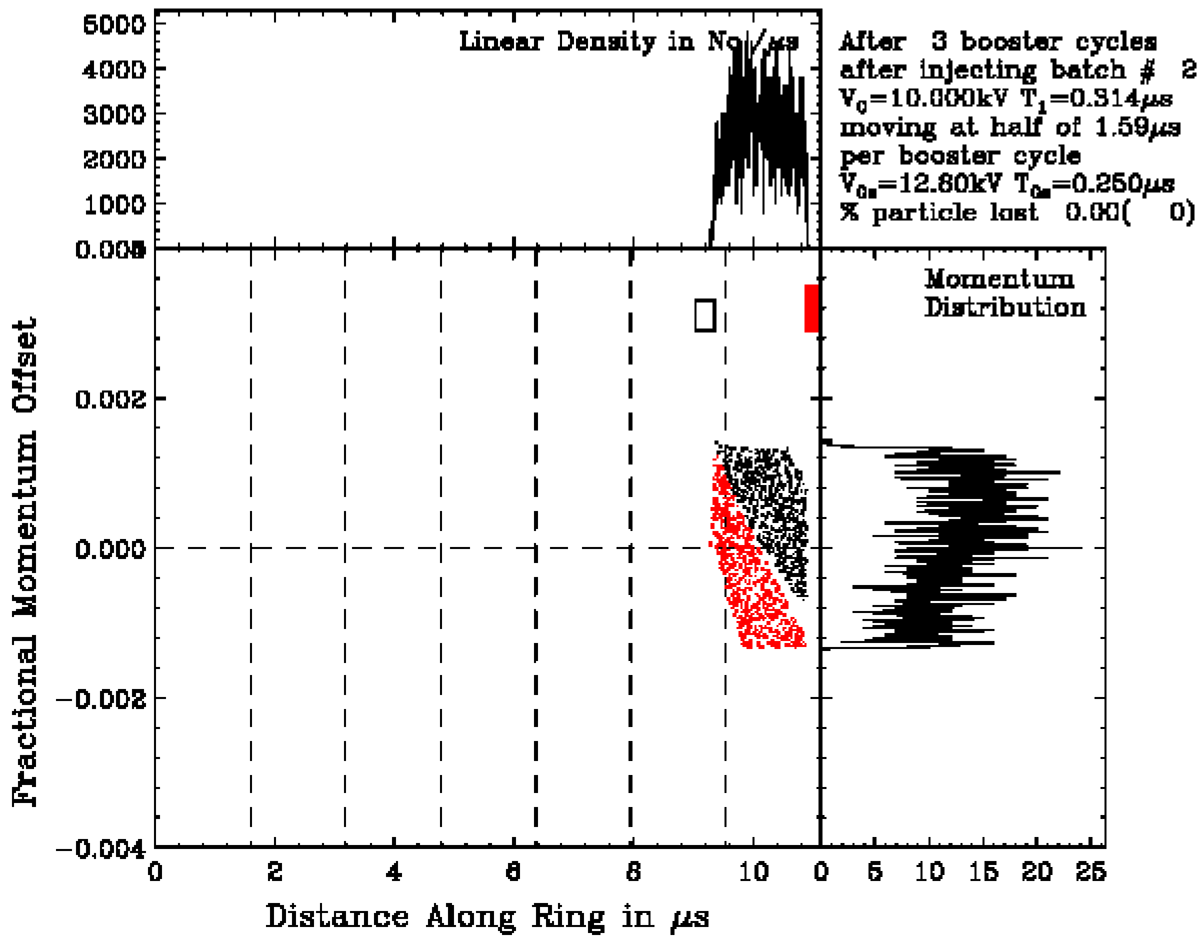

Barrier RF Experiments in the Recycler (C. Bhat)

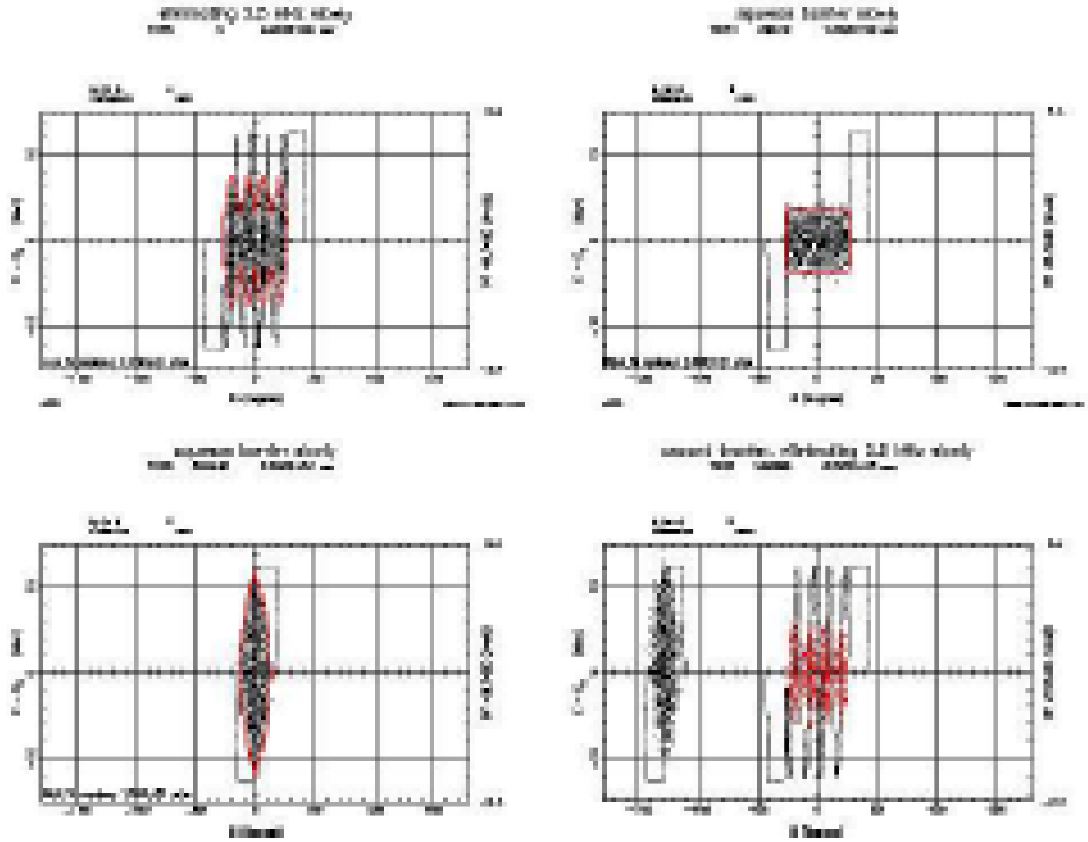

FIGURE 3. Longitudinal beam dynamics simulation results for beam stacking. Shown are distribution of beam particles in $(\Delta E, \Delta\phi)$-space. The rf wave forms and buckets are also shown. For details see the text.

Properties of Finemet (a nanocrystal magnetic alloy)

(a) Finemet vs. Ferrite (C. Ohmori et al.)

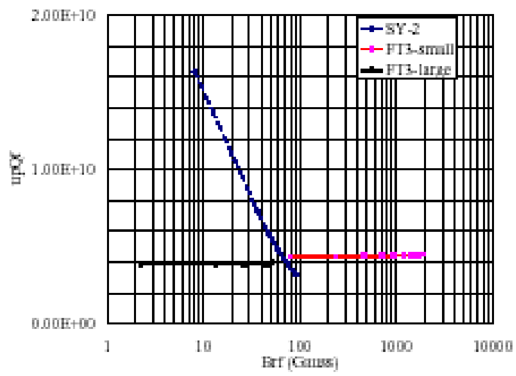

Figure 2: Magnetic flux density dependence of magnetic materials. SY2 is a typical ferrite core and the magnetic flux density dependence was observed. FT3-small and -large are MA cores of 570mm O. D. and 70 mm O.D., respectively. The MA cores have a constant shunt impedance up to 2 kGauss.

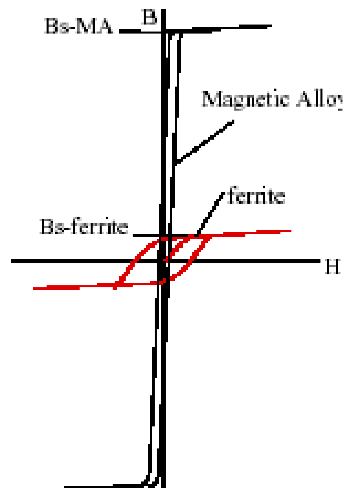

Figure 1: The hysteresis curves of magnetic materials. B_s means the saturation magnetic flux density. The usable B_{RF} is much smaller than B_s.

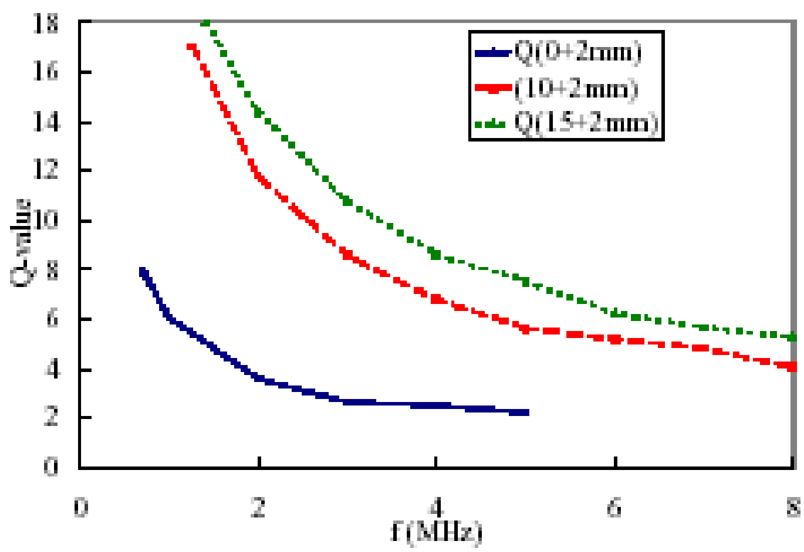

Figure 10: The Q-value of the cut core vs. gap height.

(b) Finemet (nanocrystal) vs. Metglas (amorphous) and Silicon Steel (macrocrystal) (A.W. Molvik and A. Faltens)

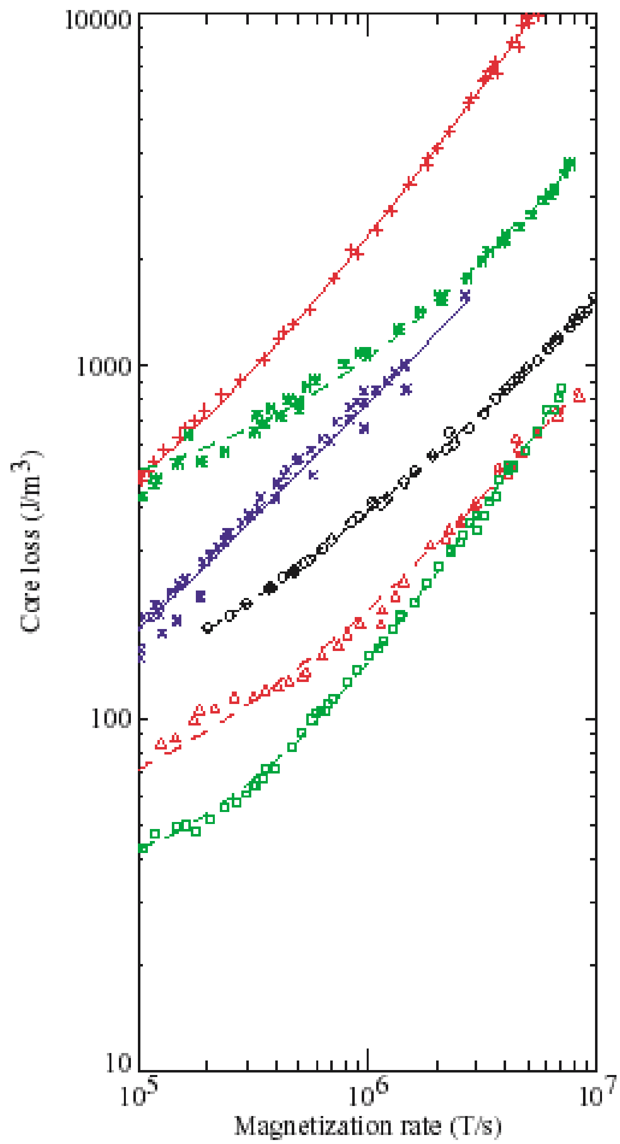

FIG. 6. (Color) Core loss versus magnetization rate for six cores, all annealed after winding. From the top, these are (+, red, solid line) 50 μm thick 3% silicon steel with $\Delta B = 3.3$ T; (*, green, dashed line) 25 μm thick 3% silicon steel with $\Delta B = 3.0$ T; (×, blue, solid line) METGLAS 2605 SA1 with magnesium methylate insulation with $\Delta B = 2.7$ T; (◇, black, dashed line) METGLAS 2605 SC cowound with mica paper insulation with $\Delta B = 2.4$ T; (△, red, dashed line) FINEMET FT-2H with $\Delta B = 2.4$ T; and (□, green, dashed line) FINEMET FT-1H with $\Delta B = 2.1$ T. Both FINEMET alloys are insulated with a glass coating.

RF Chopper Cavity made of Finemet (Fermilab/KEK)

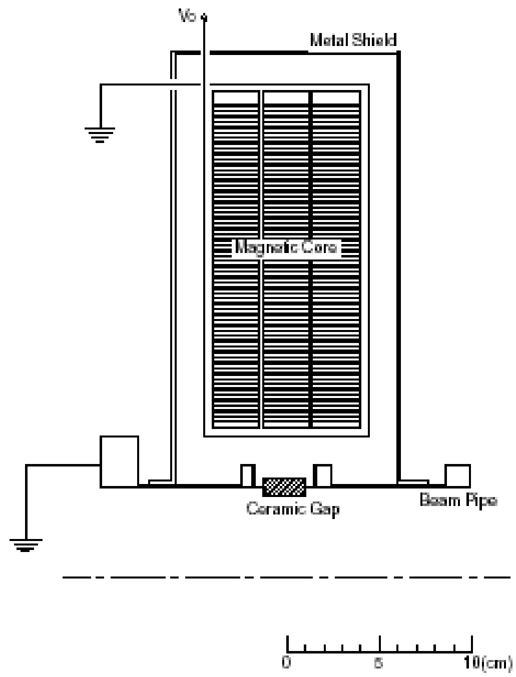

Figure 2: A test cavity used in the measurements. It consists of a magnetic core, a metal shield, a one-turn coil and a stainless steel beam pipe with a ceramic gap.

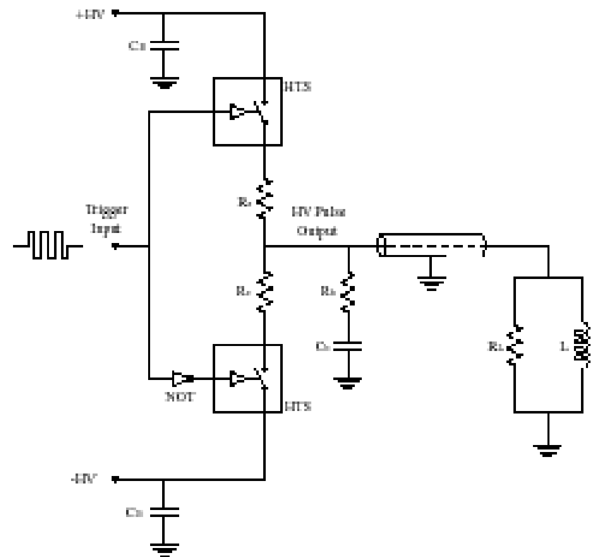

Figure 5: A circuit diagram of a bipolar (push–pull) high voltage source using two HTS transistors as the switches.

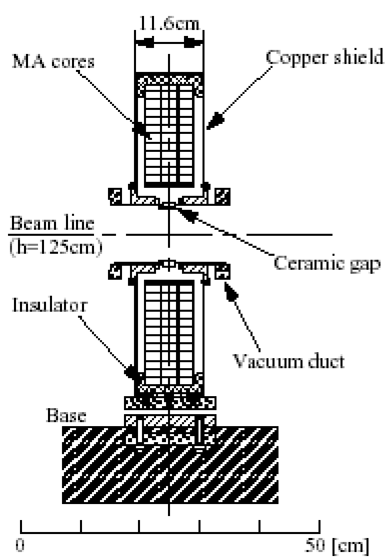

Figure 2: Side view of the chopper. Three magnetic-alloy cores with 504mm ϕ_{out} x 158mm ϕ_{in} x 25mm thickness are used. An one-turn coil is wound around the cores.

Figure 1: Chopper cavity installed at the HIMAC facility. A constant-energy beam from an ion source comes from the right-hand side, and its energy is modulated by ±5% at the chopper cavity. The downstream RFQ is located at the left-hand side, which is at the other side of the wall.

Comparison: Ferrite (4M2) vs. Finemet

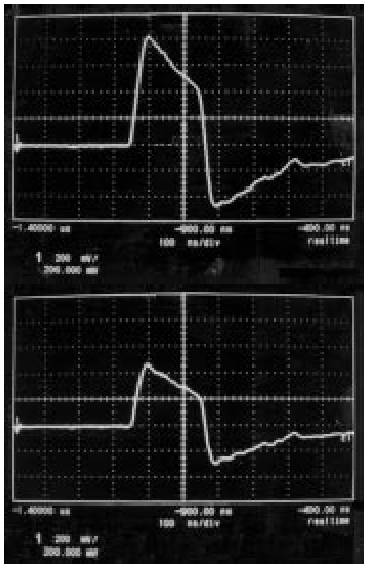

Figure 4: The primary and secondary voltage waveform when a 4M2 core is used.

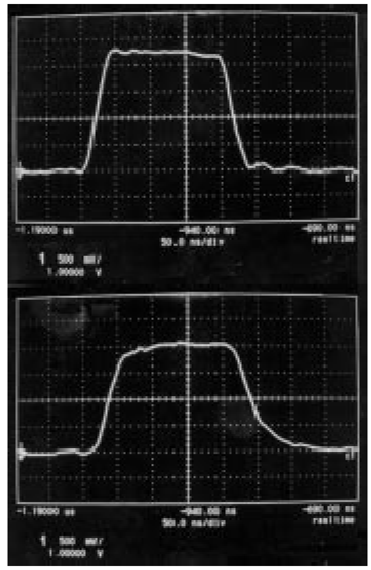

Figure 3: The primary and secondary voltage waveform when a Finemet core is used. The rise-time is about 40 ns.

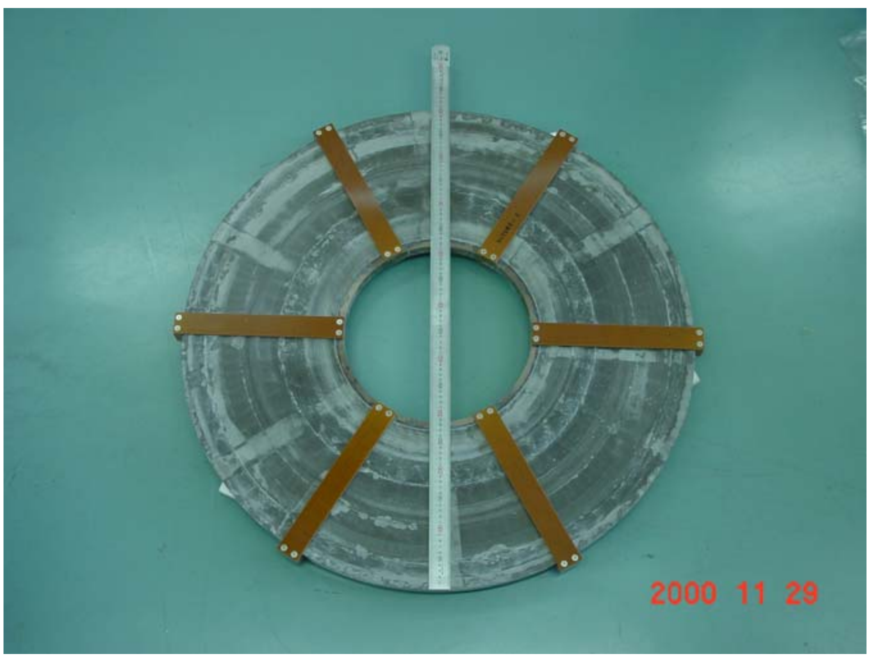

Finemet Core Design

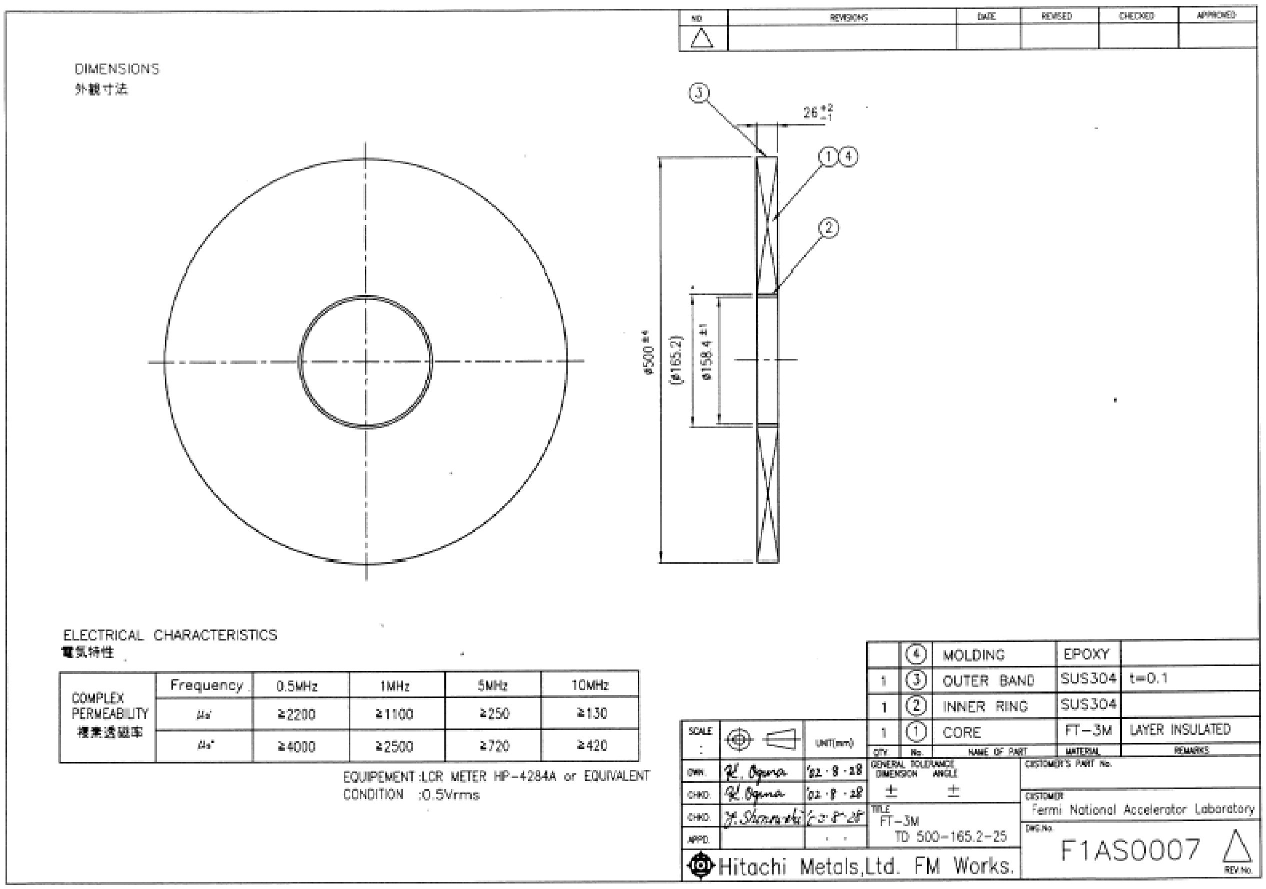

Sample Finemet Core Measurement Data

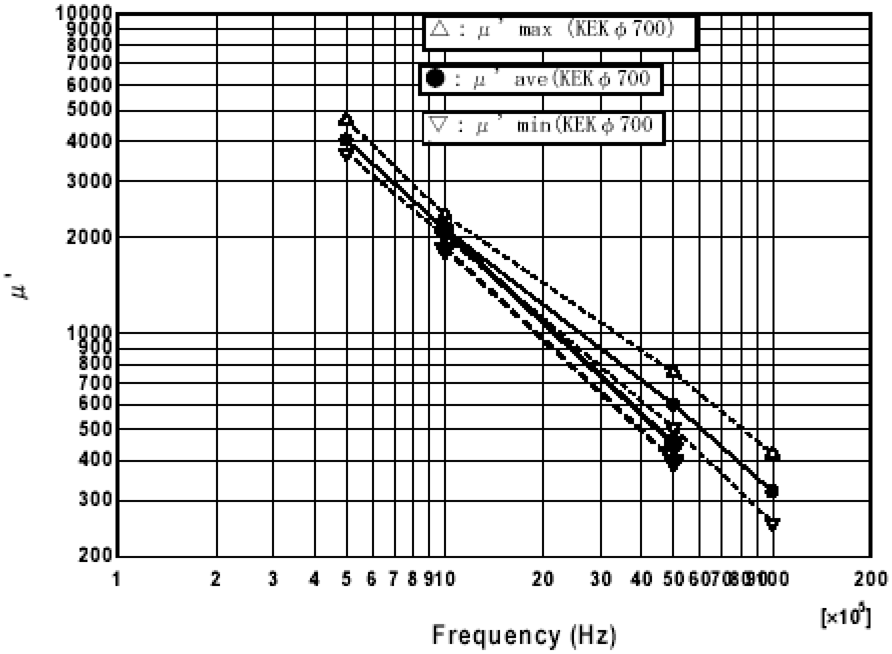

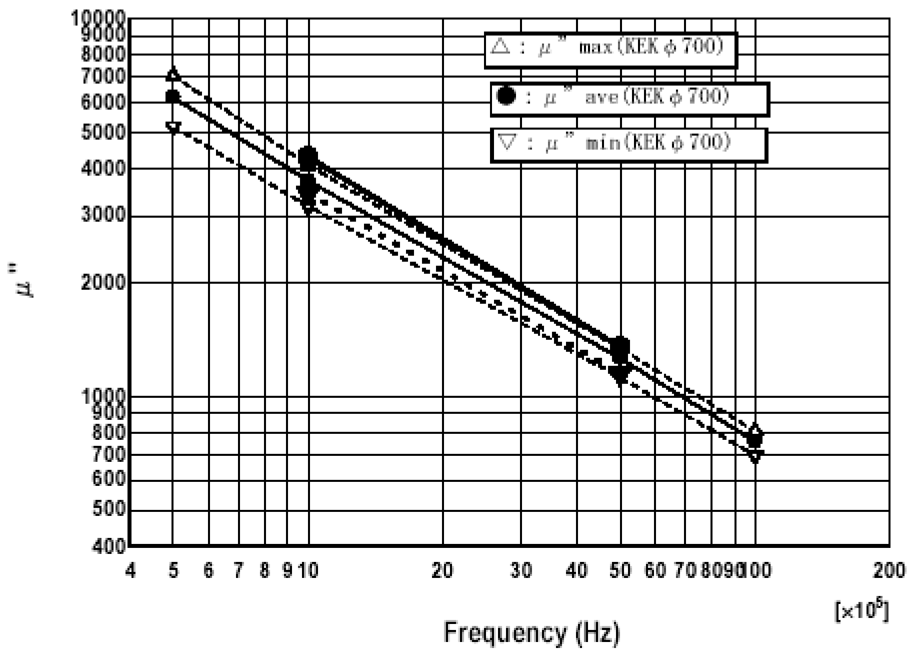

FAST HIGH VOLTAGE TRANSISTOR SWITCHES

HTS 161-06-GSM 2x16kV / 60A
HTS 301-03-GSM 2x30kV / 30A

The switching modules of the series HTS-GSM consist of two identical MOSFET switching paths, that form a so-called half bridge circuit respectively push-pull circuit. Both switching paths are controlled by a common driver, which also provides a logic signal negation for one of the switches. The switches are mutually passively locked, so that a short in the bridge is excluded under all circumstances, even then, if the control input is disturbed by electromagnetic interferences (due to bad EMC design, for example). Especially in pulse generator applications with capacitive load, the push-pull principle has considerable advantages in comparision with the conventional circuitry using a single-switch with working resistor. Push-pull circuits do not require large energy storage capacitors for a low pulse droop and, because there are no working resistor power losses, the efficiency of a push-pull pulser is excellent regardless to pulse width, frequency and duty cycle. The pulsers draw only currents for charging the connected load capacitance. Thanks to an extremely precise timing of the switches, there are also almost no cross currents in the bridge, except peak charging currents of the switch natural capacitances.

The switches are controlled by positive going signals of 3 to 10 Volts amplitude. Fault conditions as overfrequency, thermal overload (long-term overload) and incorrect auxilliary supply set the switching path A in off-state and the switching path B in on-state. Faults are indicated as a "L" signal at the fault signal output. Without 5VDC supply both switching paths (A and B) are in off-state. That means, without 5VDC the output potential could be undefined, if the HV is still applied. To ensure a defined high voltage output potential in such cases, pull-up or pull-down resistors must be connected to the output. For further design recommendations please refer to the general instructions.

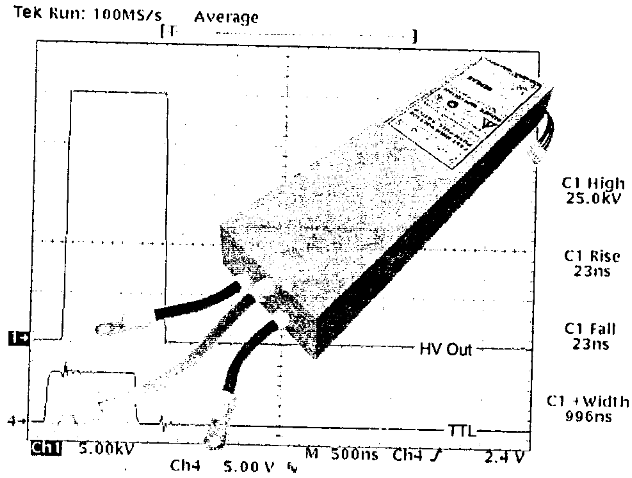

- Fast transition times, rise time and fall time ~20 ns
- Variable pulse width from 200 ns to infinity
- No pulse droop and very low ripple on the pulse top
- No working resistor power, small buffer capacitors

PUSH-PULL - Patented - Made in Germany **MOSFET TECHNOLOGY**

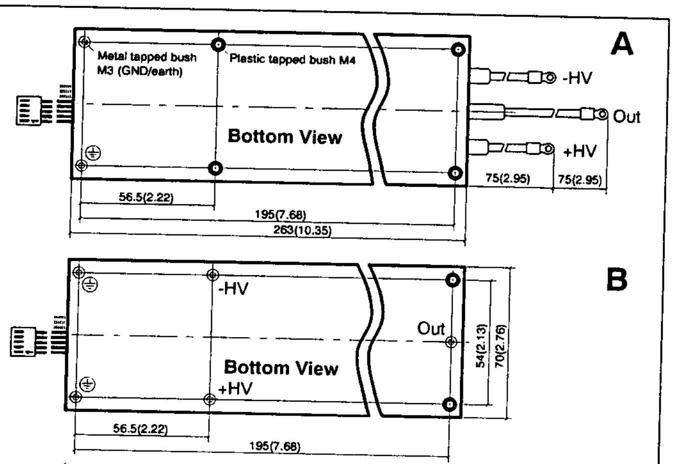

All dimensions in mm and (inch). Metric screws are included in delivery. Customized cases on request.

Test Circuit

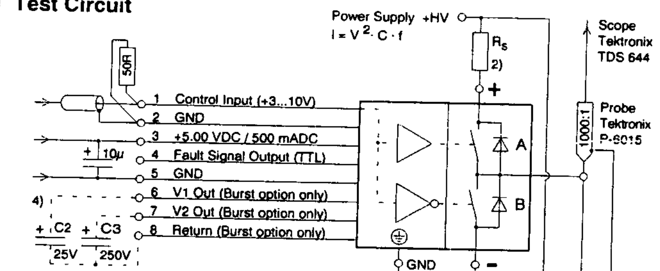

NOTES:
1) A good low impedance linkage between logical GND and earth is very important for an interference-proof operation with high switching speeds. In floating circuits a HV coupling capacitor of ~10 nF is used instead of the galvanic linkage.
2) Series resistors Rs are used for damping and short protection. All specifications refer to Rs=33 Ohm (AB, pulse proof, 1kV/2W). According to individual requirements, Rs can be between 0 and ~1M. Rs must however always be chosen so high that ringing is avoided !
3) CB should be at least 10...100 times of CL for shortest transition times.
4) Burst option only. C= 0.1µF x number of pulses per burst. C2=25V, C3=250V.

Basic Circuits

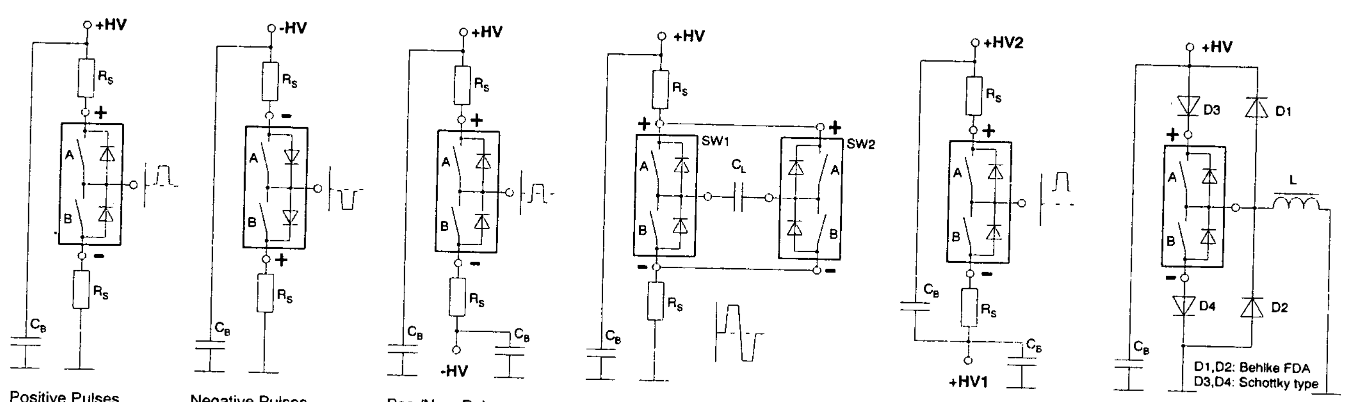

Positive Pulses

Negative Pulses

Pos./Neg. Pulses — The sum of I+HVI and I-HVI must not exceed Vo(max).

Full Bridge Circuit — Control signal for SW2 is negated.

Floating Pulser (Pos.) — HV1 + HV2 must not exceed the Max. Isolation Voltage!

Inductive Load — External diodes must be used to avoid reverse currents trough internal diodes!

BEHLKE ELECTRONIC GMBH · Am Auernberg 4 · 61476 Kronberg/Germany
+49 (0) 6173-929020, Fax +49 (0) 6173-929030, e-mail info@behlke.de, www.behlke.de

BEHLKE

TECHNICAL DATA

Specification	Symbol	Condition / Comment	161-06-GSM	301-03-GSM	Unit
Maximum Operating Voltage	$V_{O(max)}$	I_{off} < 10 µADC	2 x 16	2 x 30	kVDC
Minimum Operating Voltage	$V_{O(min)}$	Increased transition times below 0.1 x $V_{O(max)}$	0		kVDC
Typical Breakdown Voltage	V_{br}	Static voltage, I_{off} > 1 mADC, , T_{case} = 70 °C	2 x 18	2 x 36	kVDC
Galvanic Isolation Voltage	V_I	Standard plastic case (see note 1) Option 08A (Pigtail version only, see drawing A) Option 08B (Pigtail version only, see drawing A)	25 40 80	40 - 80	kVDC
Maximum Peak Current	$I_{P(max)}$	T_{case} = 25°C; t_p<10 µs, duty cycle <1%	2 x 60	2 x 30	ADC
Max. Continuous Load Current	I_L	T_{case} = 25°C: Standard plastic case (see note 1) T_{fin} = 25°C: Opt.03, increased thermal conductivity Opt. 04, cooling fins (air >4m/s)	2 x 0.7 2 x 0.86 2 x 2.2	2 x 0.33 2 x 0.41 2 x 1.05	ADC
Static On-Resistance	R_{stat}	T_{case} = 25°C: 0.1 x $I_{P(max)}$ 1.0 x $I_{P(max)}$	2 x 18 2 x 40	2 x 72 2 x 180	Ω
Maximum Off-State Current	I_{off}	0.8xV_O, T_{case}= 25...70°C, reduced I_{off} on request	10		µADC
Propagation Delay Time	t_d	Resistive Load	190		ns
Typical Output Transition Time (Rise Time & Fall Time)	t_r, t_f	0.8 x V_O 10-90%: R_S = 33 Ω, C_L = 10pF R_S = 33 Ω, C_L = 50pF R_S = 33 Ω, C_L = 100pF R_S = 33 Ω, C_L = 200pF R_S = 22 Ω, C_L = 1000pF	10 15 17 25 60	20 35 50 90 230	ns
Minimum Output Pulse Width	$t_{p(min)}$	Reduced output pulse width on request.	200		ns
Maximum Output Pulse Width	$t_{p(max)}$		No limitation, up to ∞		
Minimum Pulse Spacing	$t_{ps(min)}$	(Switch recovery time)	400		ns
Typical Output Pulse Jitter	t_j	V_{aux}=5.0 VDC: Fixed switching frequency, >2kHz V_{tr} =5.0 VDC: Sweeped frequency, <2kHz	0.1 5		ns
Max. Continuous Switching Frequency	$f_{(max)}$	Please note possible $P_{d(max)}$ limitations. Increased switching frequency on request.	2		kHz
Maximum Burst Frequency	$f_{b(max)}$	Use option 01 for >10 pulses per 20µs burst	2.5		MHz
Maximum Continuous Power Dissipation	$P_{d(max)}$	T_{case} = 25°C: Standard plastic case (see note 1) T_{fin} = 25°C: Opt. 03, incr. thermal conductivity Opt. 04, air speed >4m/s (s. note 2)	2 x 20 2 x 30 2 x 200		Watts
Linear Derating		Above 25 °C: Standard plastic case Opt.03, incr. thermal conductivity Opt. 04, air speed >4m/s	2 x 0.44 2 x 0.66 2 x 4.44		W/K
Operating Temperature Range	T_O		-40...70		°C
Typical Natural Capacitance	C_N	Capacitance between the terminals of <u>one</u> switch path: 0.1 x $V_{O(max)}$ 0.8 x $V_{O(max)}$	< 90 < 30		pF
Typical Coupling Capacitance	C_C	Both switches against ground respectively control	< 30		pF
Reverse Recovery Time of the intrinsic diodes (parasitic MOSFET diodes)	t_{rrc}	**Important Note:** Due to the high t_{rrc} of the parasitic diodes any current reversal must be avoided! Unclamped inductive load or high stray inductance of wiring may cause a short circuit in the bridge. Danger of irreparable damage! Use serial resistors, snubbers or fast free-wheeling diode networks to avoid any current reversal.	500...1000		ns
Auxiliary Supply Voltage	V_{aux}	Stabilized to ± 5%	5.00		VDC
Auxiliary Supply Current	I_{aux}	@f_{max}, (Limitation of approx. 1 A recommended)	600		mADC
Control Signal	V_{tr}	>3VDC recommended for low jitter	3...10		VDC
Fault Signal Output		Short circuit proof, source/sink current max. 10 mA: Ready = High Fault = Low	≥4.0 ≤0.8		VDC
Dimensions	LxWxH	Standard case (Without pigtails & opt. cooling fins)	263x70x35		mm³
Weight		Standard plastic case With option 04 (cooling fins in standard size)	800 1450		g

Notes:

1) The standard case is „A" for the HTS 301-03-GSM and „B" for the HTS 161-06-GSM. Please refer to the drawing overleaf. Version „B" is optionally also available for the HTS 301-03-GSM (option 06) but only in connection with additional isolation measures (e.g. oil immersion) or in case of operating voltages less than 20 kVDC. The version "B" for attachment on printed circuit boards is preferred in high speed circuits with transition times in the order of 10 to 20 ns or in case of critical EMC aspects.
2) Cooling fins are not recommended if the HTS 301-03-GSM shall be operated in air above 20 kVDC. No limitations if operated in oil. Please consult factory for further oil cooling information.

Ordering Information

HTS 161-06-GSM	Push-pull transistor switch
HTS 301-03-GSM	Push-pull transistor switch
Option 01	High frequency burst
Option 03	Increased thermal conductivity
Option 04	Non-isolated cooling fins (oil immersion for Vo >20 kV)
Option 05	High power metal case (on request)
Option 06	Printed circuit board version of HTS 301-03-GSM.
Option 08A	40kV isolation for HTS 161-06-GSM (pigtail version „A" only)
Option 08B	80kV isolation (pigtail version „A" only)

Further data and mechanical drawings are available on request. All data and specifications subject to change without notice.

Appendix. RF Cavity made of Finemet in the Main Injector
(D. Wildman)

FIGURE 7. A 7.5 MHz Finemet rf cavity installed in the Fermilab Main Injector.